HELICOPTER ENGINE-IN-THE-LOOP TEST SETUP

M. Kerler, J. Hönle, W. Erhard, H.-P. Kau †
Institute for Flight Propulsion, Technische Universität München
Boltzmannstr. 15, 85748 Garching, Germany
martin.kerler@tum.de

Computer-based simulations are often used today during the development process of new systems. Depending on the system, there is a point sometimes when computer-based simulations alone are no longer sufficient. Beyond this point, the required testing of the system prior to product launch can be furthered by using hardware-in-the-loop (HIL) systems. This paper describes a HIL system consisting of a real helicopter turboshaft engine and a helicopter flight dynamics simulation. As the term HIL is usually used for describing controller testing, the whole system is renamed by the term engine-in-the-loop (EIL). Nevertheless, it can also be used for evaluating new engine controller concepts. Another application involves the analysis of the differences in dynamic behavior of a virtual and real engine in real-time and using the EIL for educational purposes. The institute's existing testbed with an Allison 250-C20B engine was used for the realization of the EIL. An electric dynamometer simulates the loads of the helicopter rotors. The engine controller consists of a controller model running on a real-time computer and a fuel control unit. A non-linear flight dynamics model of the BO 105 helicopter is implemented for the helicopter flight dynamics simulation. For verification and validation of the EIL system, simple flight missions were performed and the test data were evaluated.

NOMENCLATURE AND ABBREVIATIONS

u	Longitudinal speed
v	Lateral speed
w	Vertical speed
$\boldsymbol{A}, \boldsymbol{B}, \boldsymbol{C}, \boldsymbol{D}$	State space model matrices
U	Input variables
X, x	State variables
Y, y	Output variables
Θ	Pitch attitude angle
Φ	Roll attitude angle
Ω	Main rotor rotational speed

AFCS	Autopilot and Flight Control System
DAQ	Data Acquisition
DLR	Deutsches Zentrum für Luft- und Raumfahrt
EDS	Engine Dynamics System
EIL	Engine-in-the-Loop
FADEC	Full Authority Digital Engine Control
HIL	Hardware-in-the-Loop
HPC	High Pressure Compressor
LPT	Low Pressure Turbine
HSS	Helicopter Simulation System
MMS	Mission Management System
MR	Main Rotor
OEI	One Engine Inoperative
SCDPS	Signal Conversation/Data Processing and Supply
SSM	State-Space Model
TOT	Turbine Outlet Temperature
VOEIO	Volitional OEI Operation

Subscripts

0	Reference
CGF	Center of Gravity Frame (Body fixed frame)

1. INTRODUCTION

The current design of medium class helicopters is primarily driven by safety reasons. For instance, helicopters in this class are twin engine powered. The engines operate under partial load for up to 60% of the helicopter mission time, however, because the power available is not needed in those cases [1]. Since the specific fuel consumption of a turboshaft engine decreases with increasing engine load, the overall specific fuel consumption can be optimized by shutting down one engine and thus increasing the engine load of the remaining engine. This procedure is only acceptable in particular flight situations. Thus, research has to be done with regard to reasonable usage of the volitional OEI operations (VOEIO). Additionally, the pilot's reaction and the helicopter's response have to be investigated in case of the running engine fails during volitional OEI flight mode.

At the institute a quick start concept of the Allison 250-C20B engine was developed and successfully tested [2]. That showed an engine start from off to

ground idle within 2.4 seconds was possible instead of a regular start time of about 25 to 30 seconds. Utilizing this quick start ability can enhance flight safety during VOEIO. As soon as an engine failure is detected of the running engine, a quick start of the engine, which was shut down before, can be performed. The pilot can perform an autorotation maneuver until the quick started engine delivers enough power to continue the flight and to conduct an emergency landing.

Before arranging any flight test, simulations have to be carried out with regard to this emergency situation. For this purpose, a non-linear BO 105 flight dynamics model was linked to a state-space model of the Allison engine [3]. Although the engine model is capable of performing quick starts, its input variables differ from the input parameter values used in real testbed quick starts because of simulation model uncertainties. Due to this issue, the simulated quick start engine has been replaced with a testbed engine using the principles of hardware-in-the-loop systems. The next section gives a general overview of the realized system. In referring to the simulation part of the system, it also provides information about the BO 105 model and its matching with transient flight test data, followed by the hardware part where the engine itself is described. The integration of all components and related issues are discussed in the subsequent section. The paper is concluded by presenting the results of a simulated flight mission and an outlook regarding future work in this field.

2. CONFIGURATION OF THE EIL SYSTEM

Flight tests offer the advantage of gaining relevant data from measurements taken of almost all helicopter components in real flight conditions. Putting new concepts or modifications to test is, however, a lengthy process. Thus, computer simulations can be applied to shorten this process and reduce risks and costs. Simulations, however, have their limits. A combination of both hardware and software can be used to overcome the shortcomings. Fig. 1 of the EIL systems shows that the software part represents the Mission Management System (MMS), the Autopilot and Flight Control System (AFCS) and the helicopter flight dynamics.

The hardware part represents the turboshaft engine at the testbed, the electric dynamometer and the engine controller. Communication between these two parts is realized by a multifunctional data acquisition system.

3. HELICOPTER SIMULATION SYSTEM

The Helicopter Simulation System (HSS) represents the BO 105 flight dynamics model as well as the MMS and the AFCS. The structure of the flight dynamics model is described in detail in [3]. Since a validation of steady flight states was conducted only at that time, the validation is extended to the transient case and a short summary is given in the next section.

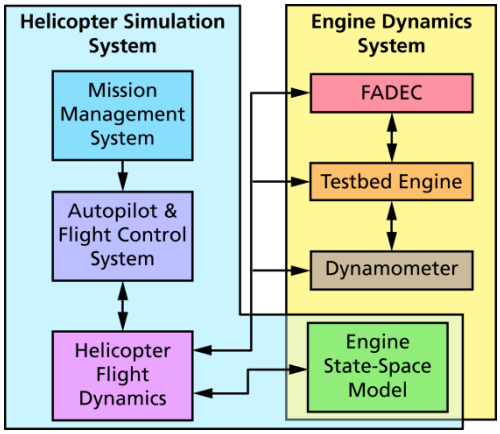

Fig. 1: Configuration of the Engine-in-the-Loop System

3.1 Helicopter Dynamics Validation

One purpose of setting up the EIL system is to load the engine with realistic power requirements depending on different helicopter flight states. Consequently, the validation of the rotor rotational speed as well as the rotor torque is one of the relevant comparisons of simulation data to flight test data. Besides that, the helicopters dynamic behavior influences the power required, too. That is why the analysis of helicopter velocities and rotational rates as well as attitudes is not negligible. As the main purpose of the helicopter dynamics model is a good representation of the powertrain dynamics and not a most accurate representation of helicopter motion dynamics, minor deviations in simulation data are absolutely tolerable regarding motion dynamics.

The flight tests were performed using the BO105 S123 research helicopter from Germany's national research center for aeronautics and space (DLR) in 1987. Its main purpose back then was to collect flight test data for system identification and simulation validation [15]. In this context, the helicopter was equipped with different sensors and in trim flight conditions it was respectively exposed to three different control input shapes. Only one control input was manipulated in each test by an input shape, thus the other control inputs stayed constant. Before the actual test, the helicopter was in trim flight at an altitude of 3000 ft and 80 kts forward speed [7]. Its gross mass was 2200 kg. In this paper, the Savitzky-Golay smoothing filter was applied to the flight test data for a better comparability due to noise reduction.

To conduct the simulation tests, the flight test input commands are referenced to zero as start value. This reference command is superposed with the

control input value of the trimmed level flight. Prior the EIL proof-of-concept tests at the Allison testbed, the dynamic behavior of the simulation model was tested using two different control input schemes: Doublet and 3211. This paper only presents and analyzes to a reasonable extent a selection of relevant parameters.

3.2 Analysis of Helicopter Response due to Doublet Control Input

This doublet control input represents a pull movement followed by a push movement of 1.5 times the travel range and then a pull movement again to reestablish the initial position of the collective stick. Fig. 2 shows the characteristic curve for the flight test and for the performed helicopter simulation.

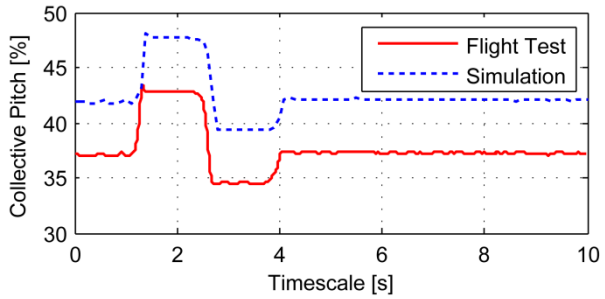

Fig. 2: Doublet input for collective pitch

Although both doublet input maneuvers start at a trimmed level flight, there is a difference of about 5% collective pitch between the recorded value of the flight test and the one from the simulation. One reason for this can be an inexact representation of the fuselage drag or the inadequately generated MR thrust of the simulation model. On the other hand, the collective pitch trim flight values of the flight test data differ between 37% and 43.5% for the same 80 kts level flight. Thus, the resulting deviation is most likely both a combination of the flight test data's accuracy and the quality of the simulation model.

The following two figures outline the change in the helicopter's attitude due to the doublet input. Fig. 3 shows the roll attitude Φ in degrees of the helicopter.

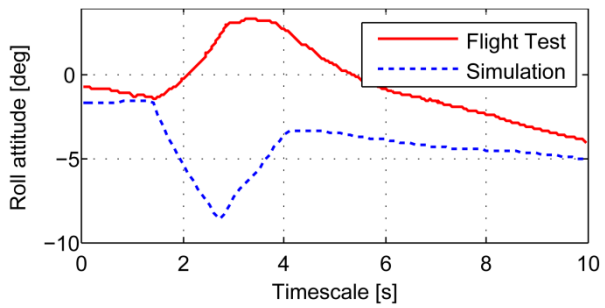

Fig. 3: Flight test and simulation results of the helicopter's roll attitude angle Φ for doublet input

While the trend of both curves is similar, both do diverge. Nevertheless, the roll gaining is almost the same in absolute values. With regard to the different directions, this probably is caused by a coordinate system definition or a sign error of the fuselage inertia tensor.

The last helicopter attitude to be looked at is the pitch angle Θ in Fig. 4. The deviation at the beginning of the maneuver can be attributed to different alignments of the body frame coordinate system in respect to the north-east-down frame. On the other hand, the difference between flight test and simulation is approximately one degree which is a negligible error. Remarkable is the slight time difference of 0.5 seconds where the simulated helicopter response is delayed and pitch changes start not until two seconds on the timescale. The trend of both curves is the same unless the simulated helicopter has a lower absolute pitch change. Thus, the helicopter dynamics due to a doublet input are properly simulated considering the pitch attitude.

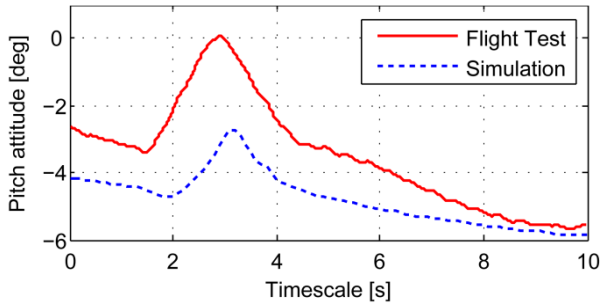

Fig. 4: Flight test and simulation results of the helicopter's pitch attitude angle Θ for doublet input

Besides the attitude changes of the helicopter, any distinguishable flight speed variations are also a matter of interest. The vertical and longitudinal velocities were chosen as selections. The first one is shown in Fig. 6, the latter one is shown in Fig. 5. As far as the flight test data are concerned, it is unknown in which exact coordinate system the speeds u and w are noted.

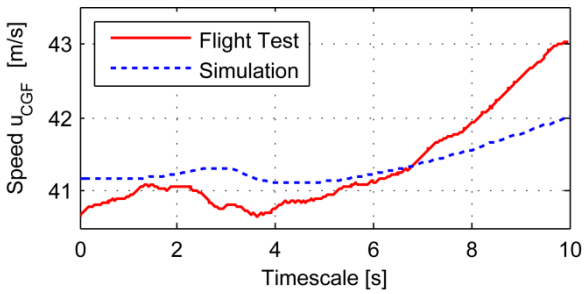

Fig. 5: Flight test and simulation results of the helicopter's longitudinal speed u for doublet input

The plotted speed curves of the simulation are noted in a separately defined body fixed frame. Looking at the speed u, the time shift of Fig. 4 can be also seen

in Fig. 5. Compared to the flight test curve, the simulation curve does not show such an increase in forward speed. An explanation could be the higher decrease of flight test pitch attitude Θ, whereby the main rotor thrust vector gets a greater longitudinal component resulting in a higher acceleration of the forward flight speed. Altogether, the simulation shows a similar behavior compared to real helicopter motion.

As the change in collective pitch directly results in thrust variation, this leads to an acceleration or deceleration of the vertical speed. Integration over time gives the related speed which is shown in Fig. 6. The vertical speed component is zero usually in trimmed level flight and regarding the north-east-down frame. However, referring to the body fixed frame and due to pitch angle, the vertical speed component is not equal to zero. The difference between the simulation model and the flight test data is up to 1 m/s in this case. But, as stated before, this can be an issue caused by a different orientation definition of the particular body fixed frames. Altogether, the curves have a similar progression. Due to pitch increase at the beginning, the helicopter experienced an increase in vertical speed replaced by a decrease due to decreasing the collective lever. As the collective pitch value is at the end of the doublet input at the same level as at the beginning, the vertical speed also levels off.

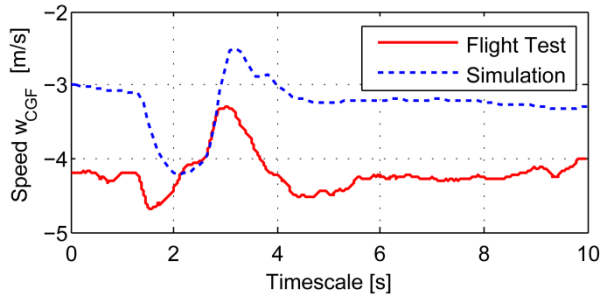

Fig. 6: Flight test and simulation results of the helicopter's vertical speed w for doublet input

Besides the helicopter's motion, the main interest is the correct simulation of the powertrain dynamics. In Fig. 7 the changes of the main rotor speed and thus the N2 speeds of the gas turbines are plotted.

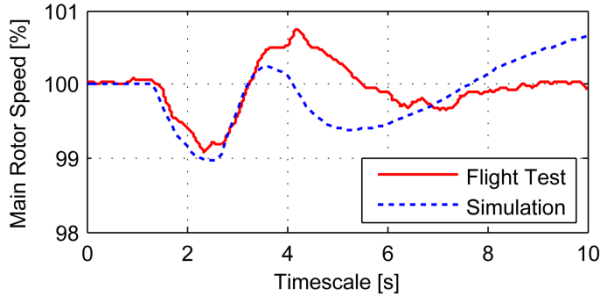

Fig. 7: Flight test and simulation results of the main rotor's rotational speed Ω for doublet input

It can be seen that the deviation from the nominal value 100% of both curves is less than 1%. At the beginning of the maneuver, the curves match one another fairly well and then start to diverge. Overall, a qualitative similar curve trend is identifiable and the simulation of the whole powertrain dynamics is satisfied at a level that is quite accurate.

The torque comparison is slightly different, however. The curve of the simulation's torque can be easily aligned with the collective doublet input, as Fig. 8 illustrates. However, the flight test curve shows a fairly smooth behavior possibly representing a slow response characteristic of the sensors. In [10] Bousman describes several difficulties regarding power measurements, though it is not absurd that the BO 105 torque measurements encountered similar problems back then.

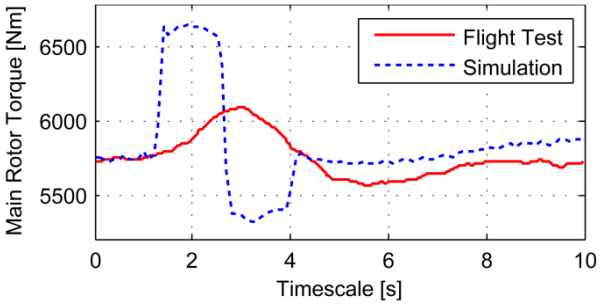

Fig. 8: Flight test and simulation results of the main rotor torque for doublet input

Due to a lack of information, the evaluation of the torque measurement data from the flight test is not practical and an interpretation of the difference between the both curves is obviously not feasible. As the required torque is an important part of the helicopter powertrain dynamics, the difference between the simulated and measured values has to be investigated further. In case of the EIL test setup, the good matching of the rotational speed was considered as sufficiently accurate. That is why the helicopter dynamics model was not modified with regard to its dynamic behavior.

4. ENGINE DYNAMICS SYSTEM

The Engine Dynamics System (EDS) consisted of an Allison 250 testbed engine with engine controller, electrical dynamometer and a real-time capable state-space model of the turboshaft engine. Due to previous research projects, the testbed engine was equipped with additional sensors and the original bleed air valve was replaced by an internally developed controllable valve as well as a fuel flow control unit. The latter is a full authority digital engine controller (FADEC) which was developed using MathWorks Matlab/Simulink and operates on a real-time computer [6].

4.1 Testbed Engine

The Allison 250 is a turboshaft engine which has several applications as helicopter or turboprop drive train. The one at the institute is the model version C20B, capable of delivering approximately 300 kW of maximum continuous power and was formerly installed in a BO 105 helicopter of the German armed forces. Today, several modified and optimized versions of the engine are still in production at Rolls Royce North America, who acquired the original manufacturer Allison.

The engine itself is of modular design with two spools. The air mass flow enters the engine by a short inlet followed by a combined seven-stage axial/radial high pressure compressor (HPC). Then, the air mass flow is guided by two ducts around the engine's center to the rear, flowing into a single reverse-flow combustion chamber. After combustion, the hot gas enters a two-stage axial high pressure turbine (HPT) followed by a two stage axial low pressure turbine (LPT), where it almost expands to ambient pressure. The HPT drives the HPC via the high pressure shaft N1 and the auxiliaries via a gearbox. The useful shaft power is provided by the LPT via the low pressure shaft N2 and a reduction gearbox.

As the institute's engine is used for different research activities, it is equipped with additional sensors compared to the normal operation instrumentation. An overview of the installed instrumentation is shown in Fig: 9.

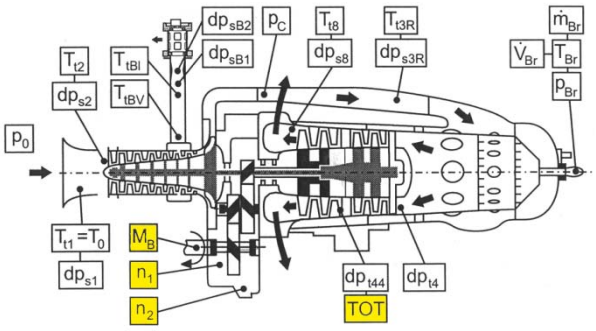

Fig. 9: Overview of the testbed's engine instrumentation [5]

The usual operation instrumentation is marked with yellow and covers the rotational speeds of both shafts N1 and N2, the engine torque as well as the turbine outlet temperature (TOT). Engine oil pressure and temperature are also normal operation instrumentation, but are not indicated in Fig. 9. Low temperatures as ambient temperature, compressor inlet temperature, bleed air temperature, compressor inlet temperature, exhaust gas temperature and fuel temperature are measured using Pt100 sensors. High temperature areas such as the section between HPT and LPT are covered by NiCr-Ni thermocouples. For recording the ambient pressure, a gauge pressure sensor was used. Other pressure metering points were realized with differential pressure sensors. Torque provided by the engine was recorded using the engine's internal torque metering device. Air mass flow rates of the inlet and bleed section were determined via venturi tubes. Fuel flow was measured by a turbine flow meter for dynamic measurements and by a scale for static measurements. An amplifier transforms the sensor's voltage signal to the common voltage range of 0 to 10 V. After signal conditioning, the voltage signal was provided to different A/D converters for measurement and to a hard-wired monitoring security system. The latter one is a backup system for emergency engine shutdowns due to any violation of several operational limits like maximum TOT or N1 overspeed. The actual measurement system can be broken down into three major parts. The first one is for continuous monitoring (Continuous Data Acquisition System) and measurement of stationary operating points (Steady State Data Acquisition System) with respect to high accuracy and low time resolution. The second one offers a total sampling rate of 200 kHz and allows the recording of transient engine operations (Dynamic Data Acquisition System). The third one is the measuring device of the FADEC with its own hardware. The collected measuring data are sent to a bus system. A server program on a single board computer processes the data for transmission over Ethernet. Members of the Ethernet network are a server for storing measurement data and a personal computer for data visualization during engine test runs [4]. A general overview of the system is given in Fig. 10.

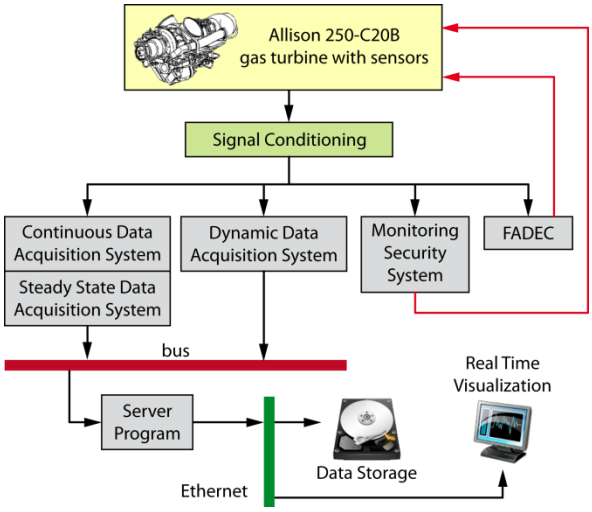

Fig. 10: Sensor data aquisition system

In addition to the extensive instrumentation, some other modifications were made.

As the original hydro-mechanical fuel flow governor does not allow any practical manipulation of the metered fuel flow, a new fuel flow controller was developed. A prerequisite was time-effective controller design and testing as well as comprehensive testing options for new controller design principles. The new controller was based on the design principles of FADEC systems. Its two main parts included the controller software and the related electro-mechanical valve control unit. The first one was developed in Matlab/Simulink. After compiling into C-Code, it was loaded on the target hardware, a dSPACE real-time system. It receives measurement data and outputs the control signals for the valve control unit. Further information is provided in [8].

The original bleed valve after the 5th compressor stage was replaced by an individually developed controllable bleed valve with additional sensors for pressure and temperature measurements of the bleed air. The production engine's bleed valve operates pneumatically depending on the compressor outlet pressure [8]. It provides a sufficient compressor surge margin for a secure engine operation especially during engine acceleration and at low N1 speeds. Due to engine operational behavior improvement and compressor stability control, the individually developed bleed valve is controllable by the FADEC [8].

The helicopter rotor loads were represented by an electrical dynamometer which was connected to the power turbine shaft of the engine. The heat of the dynamometer generated due to braking was dissipated by a cooling-water loop. In comparison to hydraulic dynamometers, an advantage of the electrical dynamometer is its higher dynamic capability enabling an appropriate simulation of the helicopter rotor dynamics.

4.2 Quasi Non-linear State-space Engine Model

As the BO 105 is a twin engine powered helicopter and as there is only one testbed engine, the other engine had to be simulated. As the whole EIL setup was running in real-time, this capability was a crucial requirement for the engine simulation model. Taking quality reasons into account, a full non-linear thermodynamic model would be the best solution. It is able to calculate the relevant parameters at every operating point relating to the thermodynamic working process. Thus, the thermodynamic conservation laws have to be satisfied for constraints like rotor power balance as well as equal rotational speeds of the HPC and HPT as they are connected to the same shaft. In conclusion, a non-linear and time-invariant equation system results from the combination of mathematical models and turbo machinery component maps representing steady state and dynamic engine behavior [11]. However, such thermodynamic based models use iteration methods like Newton-Raphson for solution calculation [13]. Since convergence is not guaranteed in any case, these models are not suitable for real-time applications like controller testing or flight simulators for pilot training courses. Consequently, linearized state-space models (SSM) of gas turbines are common in this field of application [14]. The SSM uses a state vector x for describing the states of the engine like temperatures of engine parts or rotational speed of the shafts. The input vector u of the SSM contains control input data about fuel flow and the required torque. The parameters of the output vector y are arbitrary and comprise relevant data for powertrain dynamics or cockpit gauges. All three vectors are linked to one another by matrices in the system equations (1) and (2) [12]:

$$\dot{x} = \boldsymbol{A}x + \boldsymbol{B}u \tag{1}$$

$$y = \boldsymbol{C}x + \boldsymbol{D}u \tag{2}$$

In this case, $\boldsymbol{A}$ is the state matrix, $\boldsymbol{B}$ the input matrix, $\boldsymbol{C}$ the output matrix and $\boldsymbol{D}$ the feedthrough matrix. This linear equation system is valid for its linearization point and a small area around it. If the engine's operating point deviation to this linearization point gets too large, the data of y is no longer feasible. As the whole operating range of the engine cannot be described with one single linearization point, the model has to be extended. The operating range is represented by several linearization points. At each steady state values are known as well as the corresponding system matrices for the dynamics representation. Fig. 11 provides an overview of the information flow within the engine simulation model.

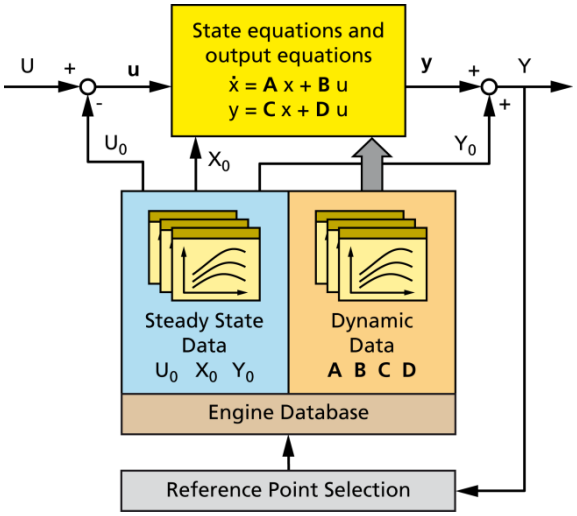

Fig. 11: Information flow of the engine simulation model [8]

A reference state of the engine was determined by analyzing the output variables Y at every simulation

time step. For this reference state, the equivalent steady state and dynamic data were calculated by linear interpolation between the two adjacent states where the dataset of the linearization was known. After determining the deviation of the actual input variables U and state variables X from the reference state (U_0 and X_0), the equations of the SSM were calculated. The result y plus the reference output Y_0 represents the new engine output data Y [8].

Parameters either experimentally recorded or calculated using fully non-linear thermodynamic models can be used for the steady state data. The latter model is required due to matrices calculation. At the institute, the software MuSYN was developed for engine performance calculations. It is capable of performing operation line calculations, off-design calculations, engine startup calculations and engine dynamics calculations as well as the generation of the quasi non-linear SSM matrices data. The program is modular based as the engine parts are represented in enclosed modules and communicated to each other via defined interfaces. Thus, MuSYN is capable of simulating all usual gas turbine configurations. Additionally, the program was recently modified to generate the quasi non-linear SSM data "with an arbitrary choice of states, inputs, outputs and linearization points" [9].

The SSM uses the same engine controller as the testbed engine to ensure comparability. As the FADEC was originally developed in Matlab/Simulink, no further integration effort was needed for the SSM control.

5. INTEGRATION ASPECTS

The HSS in Fig. 1 is entirely modeled in Matlab/Simulink and C and runs on a common personal computer in real time. The data acquisition (DAQ) system for communication between the HSS and the testbed engine is a NI-6218 USB box that was manufactured by National Instruments. It provides, among others: 32 analog inputs, 2 analog outputs, 8 digital inputs and 8 digital outputs. The I/O channels are addressed via DAQ blocks of the Simulink Data Acquisition Toolbox Block Library which reprocess the physical voltage signal of the testbed engine's Signal Conditioning System into a Simulink useable data format.

As Fig. 12 shows, the signals from the testbed (here: engine torque, the TOT, the fuel flow and N1 rotational speed as well as the engine state) are input for the Simulink subsystem Signal Conversation/Data Processing and Supply (SCDPS). In this subsystem, the voltage range signal of 0 to 10 V was converted into physical unit equivalents and vice versa. The data were multiplexed and provided to the HSS via the Testbed Engine Data bus. As output of the Simulink model, the subsystem SCDPS provides the voltage values for dynamometer torque and rotational speed of the N2.

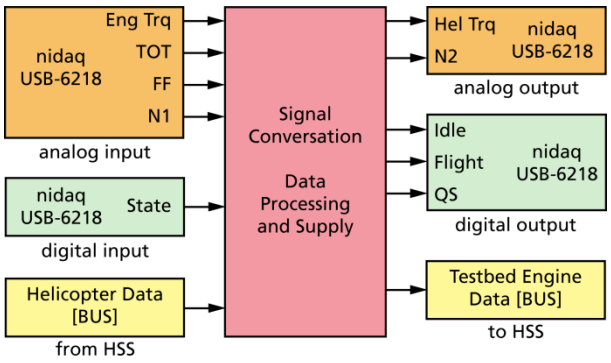

Fig. 12: DAQ integration overview

Furthermore, the subsystem addresses the engine state commands as ground idle, flight idle and quick start. The latter one is used for controlling the quick start mechanism for quick engine starts as presented in [2].

The data for the engine commands are provided by the incoming Helicopter Data bus. Since the whole EIL system is controlled by means of the HSS, no human assistance was required during the EIL runs. The FADEC was modified as it has to process engine control commands from the new external source HSS instead of the manual operator.

Besides the testbed engine, the HSS also sets the engine control commands of the state space model. Even though the state-space model of the Allison engine is part of the EDS, the HSS comprises it.

6. RESULTS

As a first proof of concept of the EIL test setup, a short flight mission was performed. The mission consisted of starting successively the engine, an initial climb maneuver, flight speed accelerations and climb maneuvers as well as performing turns followed by deceleration, decline and an landing maneuver. The resulting flight path is illustrated in Fig. 13.

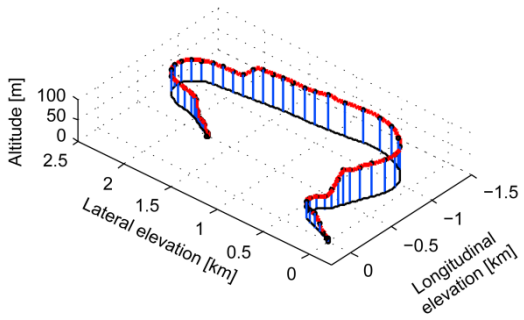

Fig. 13: Flight path of the test mission

The flight speeds attained in body fixed frame with respect to the mission time are shown in Fig. 14.

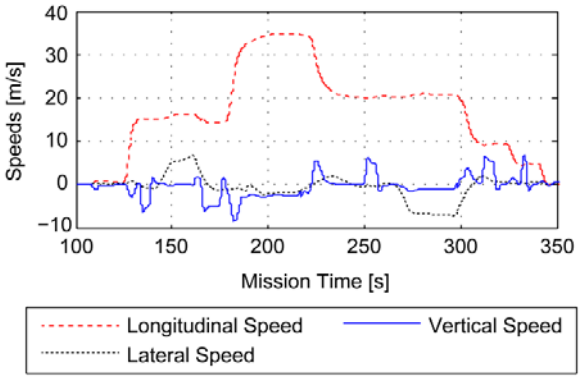

Fig. 14: Flight speeds of the helicopter in body fixed frame

Maximum flight speed was 35 m/s (68 kts) and maximum climb rate was 8.4 m/s (1653 ft/min) and sink rate 6.7 m/s (1319 ft/min). With regard to the body fixed frame, the climb rate has a negative sign whereby the sink rate has a positive one.

After a few simulation seconds, the initialization phase of the HSS model was finished and the HSS started processing the mission elements. Due to safety reasons, the starting procedure involved starting the testbed engine first and then the simulated engine. The engine start was commanded by setting the engine mode variable to 1 as seen in Fig. 15. After the engine was run up successfully, the testbed engine was kept in ground idle mode for 30 seconds to stabilize it and perform some checks. Then, the testbed engine was forced to switch into flight idle mode to be ready for following flight. Short after the HSS sets the engine mode variable of the testbed engine to 2, the engine starting procedure was performed for the simulated engine. As this one is only a simulation model, special safety checks were not performed and the simulated engine was set faster to flight mode. At the end of the whole starting procedure, the HSS was able to proceed with the actual flight mission.

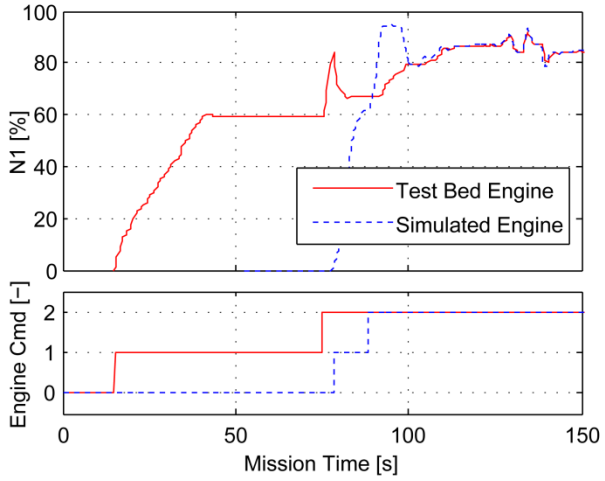

Fig. 15: Start procedure of the testbed engine and simulated engine

As the EIL offers a capability to compare the SSM with the testbed engine, the deviation from each other is a matter of interest. Fig. 16 shows the torque curve of both engines as well as the relative deviation of the simulated engine to the testbed engine. From Mission Time (MT) 120 seconds to 125 seconds a trimmed level flight is followed by a flight speed acceleration which lasts 13 seconds. The helicopters then climbs at constant flight speed to a higher altitude which ends at MT 144 seconds. Afterwards a level flight turn is performed for 20 seconds, followed by another climb maneuver.

Qualitatively the torque curves fit very well, but quantitatively there are some discrepancies. The testbed engine curve is too smooth especially with the occurrence of higher torque dynamics. This is mainly due to the testbed engine measurement rate of 2 Hz and the response time of the dynamometer as well as the response time of the fuel metering device of the FADEC and engine characteristics. In this case, deviations of up to 20% are not unusual in the areas of high engine dynamics. In areas with less engine dynamics (MT 145 seconds to 163 seconds), the quantitative deviations are minimized to almost zero. Consequently, further research has to be done due to dynamics improvement of the testbed engine incorporated in the EIL test setup.

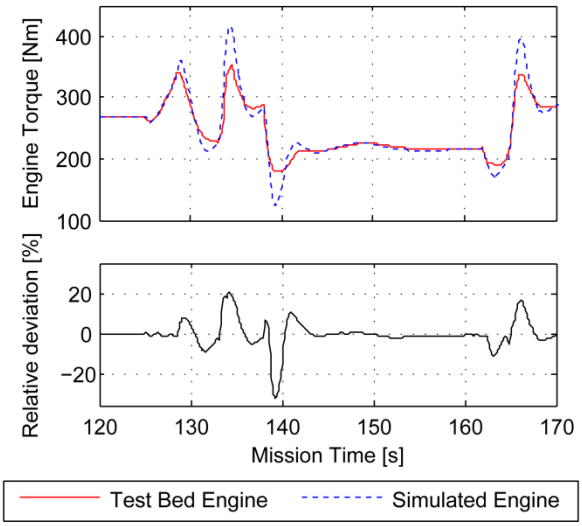

Fig. 16: Torque of the engines for different maneuvers

For the reasons mentioned above, the testbed engine is not able to provide as much torque as required by the HSS. This consequently influences the rotational speed of the rotors. Fig. 17 shows the deviation from the nominal value 100%. As usual the N2 of both engines has to be the same due to mechanical gearbox linkage and the curves in Fig. 17 have to match perfectly. With regard to this EIL test setup, this direct linkage could not be realized. Nevertheless, the qualitative curve progression is satisfactory and quantitative

differences can be caused by the low resolution of the measured data provided to the HSS.

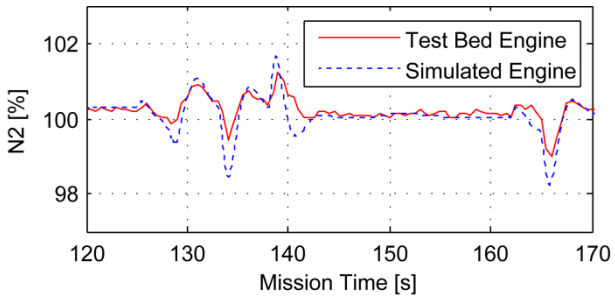

Fig. 17: N2 variation due to changing load

The relative deviation of the main rotor's rotational speed is less than +/- 2% within this MT segment. An analysis of the remaining MT comes to the same results. In most cases, the absolute deviation value is less than 1%. Thus, the lower torque dynamics of the testbed engine has no serious influence on the main rotor speed.

Besides the interaction of the testbed engine and the HSS with regard to the dynamics, a comparison between the Allison SSM and the testbed engine is also a matter of interest. For this purpose, the TOT and fuel flow were analyzed in addition to torque and rotational speed comparisons. Fig. 18 shows the TOT of both engines and the absolute deviation from each other for the MT segment.

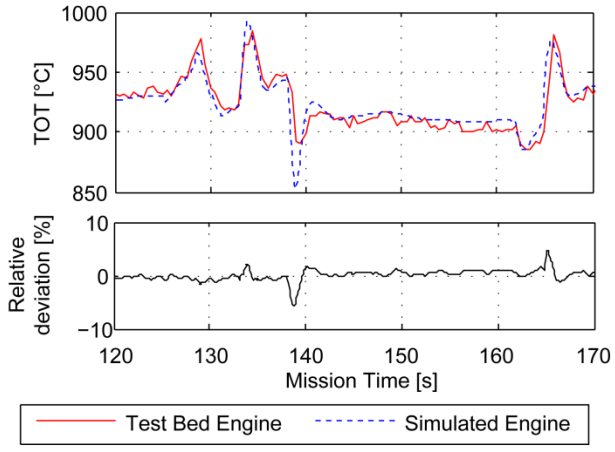

Fig. 18: TOT of the engines

The relative TOT deviation between the simulated engine and the testbed engine is very low in most time segments. If the fuel flow increases fast as can be seen at MT 138.5 seconds the deviation becomes larger. However, one has to consider the slow response characteristic of the temperature sensors as well as the non-uniform circumferential temperature distribution. All in all, the modeling accuracy of the SSM is more than sufficient with respect to the TOT.

The curves of the fuel flow as can be seen in Fig. 19 have a similar characteristic as the one belonging to the TOT. However, the relative deviation becomes greater at higher dynamics. This may be a result of the different engine torques provided due to the slow overall response characteristic of the testbed engine. On account of this, the simulated engine attempts to compensate this by providing more power and thus increasing fuel flow. This can explain the deviation peaks.

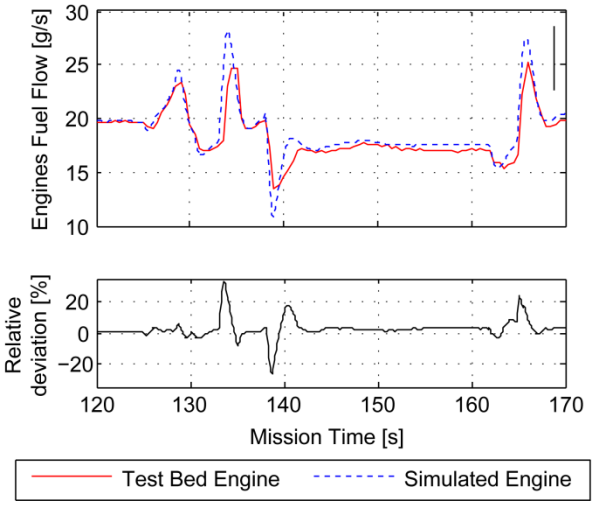

Fig. 19: Fuel Flow of the engines

7. CONCLUSION AND OUTLOOK

As described in the previous paragraphs, an EIL system was set up at the institute. It consist of a testbed engine with a sophisticated FADEC and sensor data acquisition system as well as a helicopter flight dynamics model with a mission management system and an engine state-space model representing the second engine of the simulated BO 105 helicopter. As the helicopter dynamics model has not been validated against dynamic flight test data, this has to be done to get a first impression of the model's validity. For the initial EIL setup, the helicopter dynamics are considered of sufficient quality. The FADEC was then modified to be accessible by the HSS which is an external source. To prove the overall functionality, a short helicopter flight mission was performed and thereafter the collected data were evaluated. As result, some restrictions due to the test setup were identified which can be resolved in the next expansion stages to ensure greater fidelity.

As the EIL system was mainly setup for testing the quick start system due to engine failure during VOEIO, these tests have to be done in the future. On the one hand, such simulations can be used to prove the system's functionality. On the other hand, the VOEIO has to be accepted and tested by pilots. Therefore, the HSS can be replaced by a new sophisticated research flight simulator of the Institute of Helicopter Technology of the Technische Universität München.

8. ACKNOWLEDGEMENT

The authors would like to thank Dr. Grünhagen and Dr. Kessler from DLR for their support concerning flight test data for the BO 105 helicopter.

9. COPYRIGHT STATEMENT

The authors confirm that they, and/or their company or organization, hold copyright on all of the original material included in this paper. The authors also confirm that they have obtained permission, from the copyright holder of any third party material included in this paper, to publish it as part of their paper. The authors confirm that they give permission, or have obtained permission from the copyright holder of this paper, for the publication and distribution of this paper as part of the ERF2013 proceedings or as individual offprints from the proceedings and for inclusion in a freely accessible web-based repository.

10. REFERENCES

[1] M. D. Paramour and M. J. Sapsard, *Future Technology and Requirements For Helicopter Engines*, AGARD Conference Proceedings No.302, Toulouse, France, May 1981

[2] J. Hönle, A. Barth, W. Erhard, H.-P. Kau, *Engine Quick Start in Case of Emergency - A Requirement for Saving Fuel by Means of Engine Shutdown*, ERF-049, 48th European Rotorcraft Forum, Amsterdam, Netherlands, September 4th-7th 2012

[3] M. Kerler, J. Hönle, H.-P. Kau, *Modeling of BO 105 Flight Dynamics for Research on Fuel Saving due to Single-Engine Operation,* ERF-073, 48th European Rotorcraft Forum, Amsterdam, Netherlands, September 4th-7th 2012

[4] A. Preiss, *Eintrittsstörungen bei Fluggasturbinen unter besonderer Berücksichtigung instationärer Gaszusammensetzung*, dissertation, TU München, 2001

[5] C. David, *Erstellung eines echtzeitfähigen Simulationsmodells für die Wellenleistungsgasturbine Allison 250-C20B*, diploma thesis, TU München, 1998

[6] W. Erhard, R. Gabler, A. Preiss, H. Rick, *Monitoring and Control of Helicopter Engines at Abnormal Operating Conditions*, Design Principles and Methods for Aircraft Gas Turbine Engines, RTO Meeting Toulouse, France, 11th-15th May, 1998

[7] J. Kaletka, M. B. Tischler, *Time and Frequency-Domain Identification and Verification of BO 105 Dynamic Models*, 15th European Rotorcraft Forum, Amsterdam, Netherlands, September 12th-15th 1989

[8] R. Gabler, *Betriebsverhalten von Wellenleistungsturbinen bei Verdichterinstabilitäten und Methoden zur Restabilisierung*, dissertation, TU München, 1998

[9] A. Wille, *Configuration Analysis ans Stability Improvements of the Solver and Generalisation of the Quasi Non-Linear State Space Model Generation of MuSYN*, diploma thesis, TU München, 2011

[10] W. G. Bousman, *Power Measurement Errors on a Utility Aircraft*, AHS Aerodynamics, Acoustics and Test and Evaluation Technical specialists Meeting, San Francisco, USA, 2002

[11] M. Menrath, *Experimentelle Kennwertermittlung und Systemanalyse bei Hubschrauber-Gasturbinen*, dissertation, TU München, 1989

[12] G. G. Kulikov, H. A. Thompson (eds.), *Dynamic Modelling of Gas Turbines*, Springer, London, New York; 2004.

[13] J. Kurzke, *About Simplifications in Gas Turbine Performance Calculations*, GT2007-27620, ASME Turbo Expo 2007 Proceedings, Montreal, Canada, May 14th-17th 2007

[14] K. Lietzau, A. Kreiner, Model Based Control Concepts for Jet Engines, 2001-GT-0016, ASME Turbo Expo 2001 Proceedings, New Orleans, USA, June 4th-7th 2001

[15] J. Kaletka, *BO 105 Identification Results*, Parameter Identification, AGARD Lecture Series LS-104, NATO Advisory Group for Aerospace Research & Development, 1979